

RESEARCH

Correlation among blastocoel fluid DNA level, apoptotic genes expression and preimplantation aneuploidy

Fattaneh Khajehoseini¹, Zahra Noormohammadi¹, Poopak Eftekhari-Yazdi², Hamid Gourabi³, Reza Pazhoomand⁴, Shirzad Hosseinishenatal⁵ and Masood Bazrgar³

¹Department of Biology, Science and Research Branch, Islamic Azad University, Tehran, Iran

²Department of Embryology, Reproductive Biomedicine Research Center, Royan Institute for Reproductive Biomedicine, ACECR, Tehran, Iran

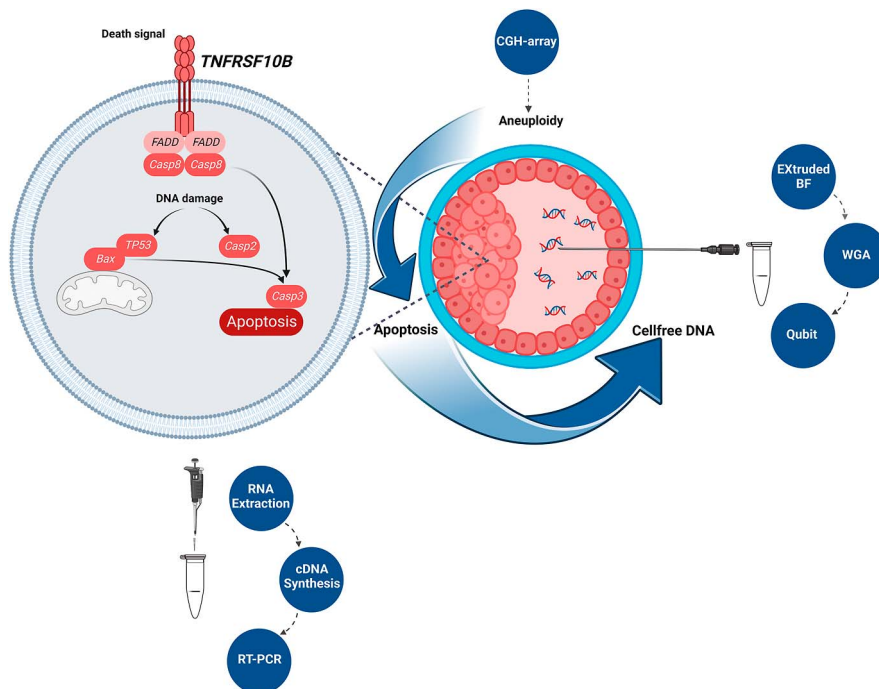
³Department of Genetics, Reproductive Biomedicine Research Center, Royan Institute for Reproductive Biomedicine, ACECR, Tehran, Iran

⁴Medical Genetics Laboratory, Shiraz Fertility Center, Shiraz, Iran

⁵Department of Embryology, Shiraz Fertility Center, Shiraz, Iran

Correspondence should be addressed to M Bazrgar: mbazrgar@royaninstitute.org

Graphical abstract



The chromosomal status of Day 5 blastocysts was determined based on trophoctoderm biopsy for all 24 chromosomes by array comparative genomic hybridization (array-CGH). The blastocoel fluid (BF) was extruded and amplified, and DNA concentration was read by a Qubit fluorometer. Apoptotic gene expression (*TNFRSF10B*, *CASP2*, *BAX* and *CASP3*) was analyzed by real-time quantitative PCR (RT-qPCR). Our findings suggest BF-DNA may be released in the blastocoel cavity of

aneuploidy blastocysts under the influence of the apoptosis mechanism, and it appears that quantifying BF-DNA has the potential to aid in the selection of viable embryos.

Abstract

It is believed that aneuploid embryos release cell-free DNA (cfDNA) into the blastocyst cavity during the self-correction process through the apoptotic mechanism. This study aimed to develop less invasive methods for predicting ploidy status by investigating how ploidy status affects blastocoel fluid DNA (BF-DNA) levels and apoptotic gene expression as indicators of embryo viability. Human blastocysts were classified into three groups; survivable embryo (SE), fatal single and double aneuploidy (FSDA) and multiple aneuploidy (MA) using array comparative genomic hybridization (array-CGH) by trophectoderm biopsy. Following BF aspiration and whole genome amplification, BF-DNA level was quantified. Apoptotic activity was assessed by measuring the genes *TNFRSF10B*, *CASP2*, *BAX* and *CASP3* using real-time quantitative PCR. Day-5 intracytoplasmic sperm injection blastocysts were scored according to the Gardner and Schoolcraft system. BF-DNA levels were significantly higher in the MA vs SE group ($P = 0.01$), while these were not statistically significant differences between the MA and FSDA groups or between the FSDA and SE groups, $P = 0.17$ and $P = 0.38$, respectively. *TNFRSF10B*, *CASP2* and *CASP3* were overexpressed in the MA and FSDA groups compared to SE, while *BAX* was downregulated. We found a significant correlation between the amount of BF-DNA and apoptosis marker genes. No significant correlation was found between embryo morphology score and BF-DNA level, BF volume or apoptosis marker gene expression levels. We observed that the correlation between apoptotic activity and BF-DNA levels is influenced by the embryo's ploidy status. These findings suggest that BF-DNA level evaluation can be applicable in selecting viable embryos for transfer.

Lay summary

Preimplantation genetic testing helps doctors choose healthy human embryos for transfer during fertility treatments, but it can be expensive, invasive and time-consuming. Recently, scientists have found a less invasive way to study embryos by looking at DNA in a fluid inside the embryo's cavity. This fluid may give us clues about how embryos try to fix problems with their chromosomes through a natural process of cell death. Our study shows that the amount of DNA in this fluid and the activity of some genes are influenced by chromosomal problems in the embryo. We also discovered that just looking at an embryo under a microscope is not enough to evaluate its genetic health. Our findings suggest that measuring the DNA in this fluid may be a promising approach for picking the best embryos for transfer.

Keywords: blastocoel fluid; aneuploidy; apoptosis; cell-free DNA; gene expression

Introduction

Human reproduction is a complex process with inherent mechanisms of natural selection that favor the development of healthy embryos. It is inherently low efficient and with increasing parental age, particularly maternal age, its efficiency decreases which can lead to infertility (Sauer 2015). Implantation failure and miscarriage are the most common causes of infertility correlated with aneuploidy in embryos (Maxwell & Grifo 2018, Hawke *et al.* 2021). On the other hand, approximately 20–80% of human *in vitro* embryos have cytogenetic imbalances, usually leading to implantation failure or early pregnancy loss (Vera-Rodriguez *et al.* 2015, Popovic 2019).

In recent years, various methods have been developed to assess and infer the genetic status of preimplantation embryos to increase the success of selecting a viable embryo and improve pregnancy outcomes.

All of these methods rely on the biopsy of embryonic cells to obtain genetic material. These methods are invasive, time-consuming and expensive and raise concerns that embryo survival may be at risk in some cases (Cimadomo *et al.* 2016, Leaver & Wells 2020). In addition, most human preimplantation embryos exhibit chromosomal mosaicism, with the most prevalent pattern of aneuploidy-diploid (Schattman 2018). Therefore, it appears that the value of predicting genetic diagnostic methods for preimplantation aneuploidy remains a controversial issue (Sermon *et al.* 2016, Gleicher & Orvieto 2017, Braude 2018, Macklon *et al.* 2019).

In recent years, the identification of amplifiable deoxyribonucleic acid (DNA) in blastocoel fluid (BF) has opened a new research field toward less invasive preimplantation genetic methods. This technique, often called blastocentesis, involves collecting samples from

this internal embryonic source. The detection of cell-free DNA (cfDNA) in nearly 90% of BF samples collected during the freezing process raises important questions about the role, purpose and function of cfDNA in preimplantation development (Leaver & Wells 2020). Chromosomal mosaicism is observed in most embryos during the early stages of division and decreases in prevalence as development progresses (Rubio *et al.* 2020, Capalbo *et al.* 2021). Comparison between the level of mosaicism and the results of laboratory fertilization indicates that some mosaic embryos can result in pregnancy and live births, suggesting aneuploidy depletion mechanisms (Greco *et al.* 2015, Fragouli *et al.* 2017, Lledó *et al.* 2017). Tobler *et al.* (2015) conducted a study to evaluate ploidy status concordance among samples obtained from blastomere, BF and trophoctoderm (TE). Their results showed that mosaic-aneuploid embryos at the cleavage stage likely differentiate into euploid blastocysts by a mechanism that directs aneuploid nuclei to the blastocoel cavity periphery (Tobler *et al.* 2015). Therefore, if cfDNA is preferentially released from aneuploid cells into the BF, the risk of a false-positive aneuploidy diagnosis through BF biopsy increases, as the DNA released into the BF would be aneuploid, while the remaining cells in the inner cell mass (ICM) might be euploid. It is believed that cfDNA is derived from apoptotic or necrotic cells. The relationship between cfDNA, apoptosis and necrosis in cancer cells has been previously investigated (Hu *et al.* 2021). Apoptosis has been described in oocytes and early embryos under laboratory conditions (Tiwari *et al.* 2015). However, during embryonic development, apoptosis appears to be a regulated and controlled process (Haouzi *et al.* 2018). It is a common occurrence in human blastocysts, typically observed following embryonic genome activation (Boeddeker & Hess 2015). Furthermore, the removal of aneuploid cells from the ICM through apoptosis and the depletion of aneuploid cells from the blastocyst stage onwards were reported in a murine chimeric preimplantation model (Bolton *et al.* 2016).

Although the extent and timing of apoptotic events during preimplantation development are crucial for embryonic growth, our knowledge of the causes, roles and molecular mechanisms that lead to the release of cfDNA in BF is still very limited. In line with the idea that apoptosis is a possible mechanism that leads to the elimination of aneuploid cells in human blastocysts, we analyzed chromosomes at the blastocyst stage, which provides the most reliable representation of the embryonic genome due to the low impact of mosaicism in blastocysts compared to the cleavage stage (Fragouli *et al.* 2011, Franasiak *et al.* 2014, Capalbo *et al.* 2017). If an embryo attempts to correct itself by releasing aneuploid cells into the blastocoel cavity through apoptosis, we would expect this response to be reflected in the amount of cfDNA released.

To investigate this, we examined the relationship between the amount of DNA in BF (BF-DNA) and the expression levels of apoptotic genes *TNFRSF10B*, *CASP2*, *BAX* and *CASP3* in blastocysts classified as survivable embryo (SE), fatal single and double aneuploidy (FSDA) and multiple aneuploidy (MA). In addition, we investigated whether the morphology score of day 5 blastocysts and the volume of fluid collected from the blastocoel cavity are associated with BF-DNA levels and the expression of apoptotic genes across the different ploidy groups.

Materials and methods

Ovarian stimulation

The ovarian stimulation protocol included a daily administration of 150 IU Gonadotropin-releasing hormone (GnRH) agonist (Merck Serono, Italy) as recombinant FSH starting from day 2 of the menstrual cycle, along with Cetrotide (Merck, France), a GnRH antagonist, at a dose of 0.25 mg/day beginning on day 6. Ovulation was triggered with 0.1 mg Decapeptyl (Ferring GmbH, Germany), a GnRH agonist and 250 µg Ovitrelle (Merck Serono, Italy) as recombinant hCG. Oocyte retrieval was performed 36 h after the ovulation trigger. This step involved collecting mature oocytes under ultrasound guidance. Before performing ICSI (intra-cytoplasmic sperm injection), the cumulus cells surrounding the oocyte were isolated. After fertilization was confirmed by the presence of two pronuclei and a second polar body, the embryos were cultured until day 5 to allow development into the blastocyst stage.

Preparation of embryos

In this study, 36 frozen human blastocysts were used, donated by 20 couples (maternal age 37.51 ± 6.19 years) who had previously undergone *in vitro* fertilization cycles with preimplantation genetic testing for aneuploidy (PGT-A) due to secondary infertility and recurrent miscarriage. All embryos were anonymized, deemed unsuitable for transfer, and obtained with informed patient consent at the time of donation. All these embryos had been cryopreserved using the vitrification technique. Evaluation of all 24 chromosomes in the embryos was conducted using array comparative genomic hybridization (array-CGH) by TE biopsy. For this purpose, the whole genome of the TE samples was amplified (REPLI-g, QIAGEN, Germany). The quality of the amplified DNA was verified by loading 5 µL of the final product onto a 1.5% (w/v) agarose gel electrophoresis. Upon confirming the quality, the amplified DNA was labeled for array-CGH, followed by hybridization, washing and scanning (Agilent Technologies, USA). Subsequently, the samples were analyzed to detect chromosome aberrations

(Agilent CytoGenomics, USA). Based on the array-CGH results, the embryos were classified into three groups; SE, FSDA and MA. The SE group consisted of embryos with partial or only one chromosome involved in aneuploidy that does not lead to preimplantation embryonic death, including cases of survivable trisomy and monosomy, such as XXY, XO, Trisomy 21, Trisomy 18 and Trisomy 13. The FSDA group included embryos with one or two chromosome aneuploidy, which have a high risk of preimplantation embryonic death. The MA group comprised embryos with multiple chromosome aneuploidy (Supplementary Table 1 (see section on [Supplementary materials](#) given at the end of the article)).

Study design

The thirty-six frozen day-5 embryos were first placed under the laboratory slow-thaw protocol. The warming methods were carried out based on the protocol used in the Royan Institute ([Michailov *et al.* 2023](#)). After warming, embryos were incubated at 37 °C in 5% O₂, 5% CO₂ and 90% N₂ conditions. Twenty-nine out of 36 of these blastocysts were expanded (29/36, 80.55%), and a blastocoel cavity was observed. Morphological assessment was carried out using the Gardner and Schoolcraft grading system ([Gardner *et al.* 2002](#)) by an experienced embryologist. On day 5, the BF was collected from 29 blastocysts ([Gianaroli *et al.* 2019](#)). In summary, each embryo was placed in a 15 µL PBS (phosphate-buffered saline, pH = 7.4) drop under mineral oil (Sigma-Aldrich, USA). The blastocysts were immobilized by a holding pipette, and the BF was collected using an ICSI needle inserted through the TE cells and from the opposite side of the ICM location to minimize the potential risk of damage and contamination with TE and ICM cells. Single aspiration of the BF was performed considering the prevention of any cellular material contamination during aspiration. The volume of BF was determined using the formula for the volume of a sphere: $V = (4\pi R^3)/3$, where R represents the radius which is usually a radius range of 80–100 µm were utilized. The aspirated BF was then transferred to 0.2 mL ‘deoxyribonuclease (DNAase)- and ribonuclease (RNase)-free’ microtubes containing 2.5 µL PBS. The bottom of the ICSI micropipette was subsequently broken into the tube to prevent material loss. Laser pulses (1-microsecond duration, Hamilton Thorne Zilos, USA) were then used to create a hole in the zona pellucida and remove the embryo from it. The embryos were then transferred to 10 µL PBS drops for washing, and after two washes, they were transferred to 10 µL Freeze-Media drops (PBS without Mg²⁺ and Ca²⁺ + 0.1% polyvinylpyrrolidone) and finally transferred to 0.2 mL DNase- and RNase-free microtubes. The day-5 embryo residues were collected for all 29 embryos. Following BF collection, blastocysts were transferred to a separate microtube containing an RNase inhibitor (Fermentas, Germany), snap-frozen in liquid nitrogen and stored at –70 °C until further processing.

The vial containing the BF was immediately subjected to whole genome amplification (WGA). The collection of BF and residual blastocysts was performed in a standard laboratory setting, following the guidelines for laboratory fertilization assays.

Weighted embryo morphology score

Embryo morphology was assessed by an experienced embryologist using the Gardner and Schoolcraft grading system ([Gardner *et al.* 2002](#)). The morphological status of the embryos was scored based on the significance of expansion blastocyst, ICM and TE cells to determine the most viable embryo, according to the following formula: ‘weighted embryo morphology score = (expansion grade × 3) + (ICM grade × 2) + (TE grade × 1)’ ([Rule *et al.* 2018](#)).

BF DNA quantification

The whole genome of the BF-DNA was amplified using the REPLI-g single-cell kit (QIAGEN, Germany), following the manufacturer’s instructions. Briefly, 2.5 µL of each sample was incubated at 30 °C for 8 h in a total volume of 50 µL with amplification kit solutions and heated to 65 °C for 3 min to inactivate DNA polymerase. The quality of the amplified DNA was assessed by agarose gel electrophoresis (1.5% w/v), and the DNA concentration was measured using the Qubit dsDNA HS kit (Thermo Fisher Scientific, USA) according to the manufacturer’s instructions. This kit quantifies DNA based on the binding of a fluorescent dye that specifically binds to dsDNA, even in the presence of other biomolecules. The amount of dsDNA was determined by measuring fluorescence intensity with a standard DNA concentration curve. After generating a standard curve, 1 µL of each amplified BF-DNA sample was independently measured using the Qubit 2.0 fluorometer (Thermo Fisher Scientific, USA).

Apoptotic gene expression

To assess the expression of apoptotic genes in the collected blastocysts, we selected four apoptotic genes that have been previously reported to be expressed in human blastocysts ([Haouzi *et al.* 2018](#)). Primers were designed using PerlPrimer1.1.21 to amplify *TNFRSF10B*, *CASP2*, *BAX*, *CASP3* and housekeeping genes actin beta (*ACTB*) and 18S ribosomal RNA (*18S rRNA*). Primer specificity was validated by Primer-BLAST, (NCBI), (Supplementary Table 2). Ribonucleic acid (RNA) extraction was performed by pooling two blastocysts of each group (based on a similar range of BF-DNA concentrations and their ploidy status) according to the manufacturer’s protocol for the PicoPure™ RNA Isolation Kit (Thermo Fisher Scientific, USA). The cDNA synthesis was performed using 10 µL total RNA and the RiboAmp RNA Amplification Kit

(Arcturus, Thermo Fisher Scientific, USA) according to the manufacturer's protocol. Finally, 2 μ L cDNA was diluted with 8 μ L nuclease-free water and prepared for real-time quantitative polymerase chain reaction (RT-qPCR). All primers were validated for amplification efficiency before sample analysis according to the minimum information for the publication of quantitative real-time PCR experiments (MIQE) guidelines, with a Pearson correlation coefficient ($r^2 = 0.98-0.99$) and amplification efficiency between 90 and 110% (Bustin et al. 2009). Real-time quantitative PCR was performed in a final volume of 15 μ L using a mixture of 3.7 μ L 2 \times SYBR Green qPCR Master Mix (Ampliqon, Denmark) and 9 μ L nuclease-free water with 0.37 μ L of each reverse and forward primer, and 1.5 μ L template cDNA in an ABI thermocycler (Applied Biosystems, USA). The genes were amplified as follows: 95 $^{\circ}$ C for 10 min, 45 cycles of 95 $^{\circ}$ C for 15 s and 60 $^{\circ}$ C for 1 min. Nuclease-free water was used for negative control reactions. Each reaction was performed in duplicate. Notably, in the primary optimizations, amplified products were observed on a 2% (W/V) agarose gel. The relative expression of selected genes was calculated using the $2^{-\Delta\Delta Ct}$ method, with *ACTB* as the reference gene.

Statistical analysis

Statistical analysis was performed using GraphPad Prism 9.5.0 software (<https://www.graphpad.com/updates/prism-950-release-notes>) and, the ANOVA test (GraphPad Software, USA). The normality of the variables within the groups was assessed using the Kolmogorov–Smirnov test. The Mann–Whitney test was then used to compare BF-DNA and weighted morphology scores across each group. Linear regression was used to determine the statistical significance between embryo morphology scores, BF-DNA concentrations, BF volume and the relative expression of apoptotic genes. $P < 0.05$ was considered to be statistically significant.

Results

BF-DNA quantification

Twenty-nine expanded embryos were classified into three groups, including SE ($n = 9$), FSDA ($n = 10$) and MA ($n = 10$) (Supplementary Table 1). The BF-DNA was successfully amplified in 93.1% of embryos (27/29). Quality control of the amplified products was performed on 1.5% (w/v) agarose gel. Considering the sensitivity range of the kit used, we considered values reported greater than 600 (ng/mL), which were read as 'sample too high' by the Qubit, to be equal to 120 ng/ μ L (the maximum value read by the kit) Table 1 represents the quantification results of three groups. The amount of BF-DNA in the MA group showed a statistically significant increase compared to the SE group ($P = 0.01$). An increase in BF-DNA was observed between the FSDA group and the SE group, and between the MA group and the FSDA group. However, these differences were not statistically significant ($P = 0.17$ and $P = 0.38$, respectively), (Fig. 1).

Apoptotic gene expression

The expression of four apoptotic genes, including *TNFRSF10B*, *CASP2*, *BAX* and *CASP3*, and the housekeeping genes, including *ACTB* and *18S rRNA* was evaluated in the SE, FSDA and MA groups. Samples were normalized against the internal reference gene, *ACTB* (the *18S rRNA* gene was not used for data normalization because the Ct alterations in different samples exceeded ± 1). RT-qPCR findings revealed a significant overexpression level of the *TNFRSF10B* gene in the MA group in comparison with the SE group ($P = 0.0001$). Interestingly, we observed overexpression of *TNFRSF10B* in the MA group in comparison with the FSDA group ($P = 0.03$), and in the FSDA group in comparison to the SE group ($P = 0.0001$). Similarly, the *CASP2* gene was overexpressed in the MA group

Table 1 Amount of BF-DNA measured by Qubit and morphology score in each group of human blastocysts.

Group	BF-DNA (ng/ μ L)	Weighted embryo score	P-value*
SE			
Minimum–maximum	0.286–114		
Mean \pm SD	45.57 \pm 15.18	18.33 \pm 1.16	0.7
Median (IQR)	28.60 (4.01–88.30)	18 (15–21)	
FSDA			
Minimum–maximum	17.04–120		
Mean \pm SD	77.65 \pm 12.77	20.4 \pm 1.38	0.0009 [†]
Median (IQR)	82 (40.80–120)	21 (18–24)	
MA			
Minimum–maximum	35.2–120		
Mean \pm SD	100.44 \pm 8.23	18.5 \pm 0.93	0.0001 [†]
Median (IQR)	106 (94.80–118.5)	18 (16.50–21.25)	

BF, blastocoel fluid; SE, survivable embryo; FSDA, fatal single and double aneuploidy; MA, multiple aneuploidy.

*Mann–Whitney test. [†]Statistically significant level of 0.05.

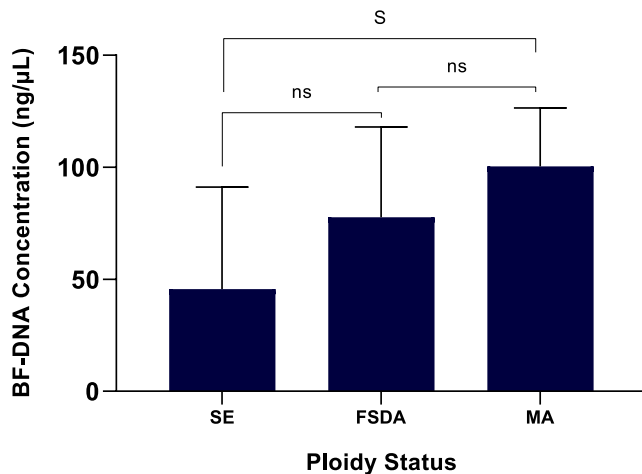


Figure 1

The amount of blastocoel fluid DNA (BF-DNA) increased in the blastocoel cavity in each group based on ploidy status as read by QUBIT. Bars represent the mean \pm SEM. S, significant difference; NS, non-significant difference.

in comparison with both the FSDA and SE groups ($P = 0.03$ and $P = 0.0001$, respectively), and was also overexpressed in the FSDA group in comparison with the SE group ($P = 0.001$). In contrast, the *BAX* gene exhibited a significantly lower expression in the MA group in comparison with the FSDA group ($P = 0.02$), and in the FSDA group in comparison with the SE group ($P = 0.01$), with the MA group showing the most downregulation compared to the SE group ($P = 0.0001$). Finally, *CASP3* gene expression was significantly overexpressed in the MA group in comparison to the FSDA ($P = 0.04$). In addition, *CASP3* was upregulated in both the MA and FSDA groups in comparison to the SE group ($P = 0.0001$ for both comparisons), (Fig. 2).

Correlation between BF-DNA concentration & apoptotic gene expression

Linear regression analysis was employed to assess the correlation between the amount of BF-DNA and the expression changes of apoptotic genes across all three groups in our study (Fig. 3). The analysis revealed a significant positive correlation between BF-DNA concentration and the expression levels of *TNFRSF10B*, *CASP2* and *CASP3* genes, with correlation coefficients as follows: (BF-DNA = $31.82 + (15.61 \times TNFRSF10B)$; $R^2 = 0.25$; $P = 0.004$), (BF-DNA = $7.85 + (51.26 \times CASP2)$; $R^2 = 0.13$; $P = 0.04$) and (BF-DNA = $31.76 + (16.53 \times CASP3)$; $R^2 = 0.28$; $P = 0.002$). Conversely, an inverse correlation was observed between BF-DNA level and *BAX* gene expression, as indicated by the following model: (BF-DNA = $136.4 - (74.93 \times BAX)$; $R^2 = 0.20$; $P = 0.01$).

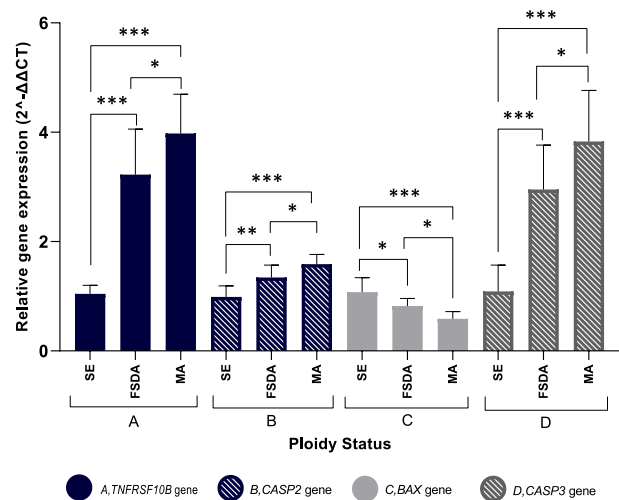
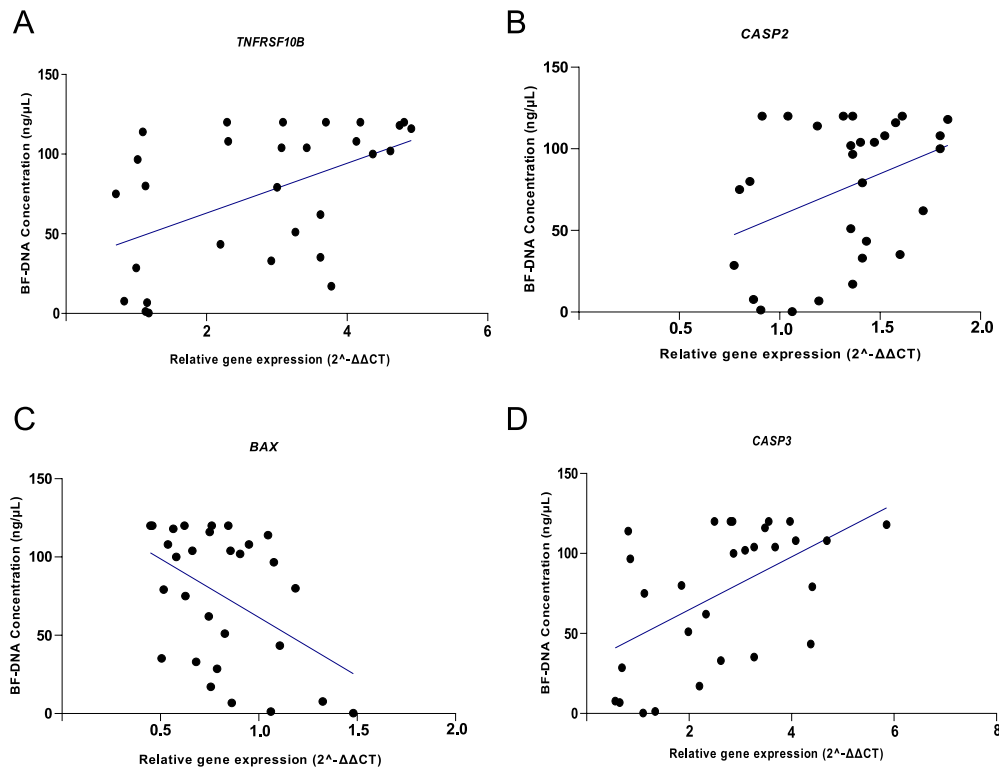


Figure 2

Expression of apoptosis genes in human preimplantation blastocysts. The RT-qPCR data showed; that (A) *TNFRSF10B* is overexpressed in the MA group compared to both FSDA and SE ($P = 0.03$ and $P = 0.0001$, respectively), and also increased in the FSDA group compared to SE ($P = 0.0001$). (B) *CASP2* is upregulated in the MA group compared to both FSDA and SE ($P = 0.03$ and $P = 0.0001$, respectively), and also overexpressed in the FSDA group compared to SE ($P = 0.001$). (C) *BAX* is downregulated in the MA group compared to both FSDA and SE ($P = 0.02$ and $P = 0.0001$, respectively), and also downregulated in the FSDA group compared to SE ($P = 0.01$). (D) *CASP3* is overexpressed in the MA group compared to both FSDA and SE ($P = 0.04$ and $P = 0.0001$, respectively), and also in the FSDA group compared to SE ($P = 0.0001$). Symbols indicate significance: * $P < 0.05$, ** $P < 0.001$, *** $P < 0.0001$.

Correlation between BF-DNA concentration & weighted embryo score

Table 1 presents the mean weighted embryo scores for each group, calculated using the previously described algorithm (Rule et al. 2018). No significant relation was observed between the mean morphology scores and mean BF-DNA in the SE group ($P = 0.7$). However, a significant relation was observed between the mean morphology scores and mean BF-DNA in the FSDA and MA groups ($P = 0.0009$ and $P = 0.0001$, respectively). Analysis of the correlation between BF-DNA concentration and weighted embryo scores did not reveal a significant association ($P = 0.9$), (BF-DNA = $70.48 + (0.2644 \times \text{score})$; $R^2 = 0.00$). Similarly, the correlation between weighted embryo scores and gene expression levels of *TNFRSF10B*, *CASP2*, *BAX* and *CASP3* in the SE, FSDA and MA groups was not significant ($P > 0.05$). The regression equations for these correlations were as follows: (weighted embryo score = $18.46 + (2.557 \times TNFRSF10B)$; $R^2 = 0.01$; $P = 0.5$), (weighted embryo score = $19.42 - (0.1915 \times CASP2)$; $R^2 = 0.00$; $P = 0.9$), (weighted embryo score = $17.85 + (1.590 \times BAX)$; $R^2 = 0.01$; $P = 0.5$) and (weighted embryo score = $18.96 + (0.08027 \times CASP3)$; $R^2 = 0.00$; $P = 0.8$).

**Figure 3**

Scatter plots of the apoptosis gene expression against BF-DNA concentration for all 29 embryos. There was a significant positive correlation between the concentration of BF-DNA and the expression of the *TNFRSF10B*, *CASP2* and *CASP3* genes and a significant inverse correlation with the *BAX* gene. (A) Scatter plot of *TNFRSF10B* gene against BF-DNA concentration (BF-DNA = $31.82 + (15.61 \times TNFRSF10B)$; $R^2 = 0.25$), ($P = 0.004$). (B) Scatter plot of *CASP2* gene against BF-DNA concentration (BF-DNA = $7.853 + (51.26 \times CASP2)$; $R^2 = 0.13$), ($P = 0.04$). (C) Scatter plot of *BAX* gene against BF-DNA concentration (BF-DNA = $136.4 + (-74.93 \times BAX)$; $R^2 = 0.20$), ($P = 0.01$). (D) Scatter plot of *CASP3* gene against BF-DNA concentration (BF-DNA = $31.76 + (16.53 \times CASP3)$; $R^2 = 0.28$), ($P = 0.002$). These findings indicate that increased BF-DNA levels are associated with the upregulation of *TNFRSF10B*, *CASP2* and *CASP3* genes while correlating with the downregulation of the *BAX* gene.

Retrieved BF volume

The BF volume obtained from each embryo was approximately 0.001 μ L. No significant correlation was found between BF-DNA concentration and the volume of BF ($P = 0.4$), (BF-DNA concentration = $87.85 - 8,800 \times$ volume; $R^2 = 0.02$). Correlation analysis between BF volume and the expression levels of *TNFRSF10B*, *CASP2*, *BAX* and *CASP3* genes also did not reveal significant associations ($P > 0.05$). The regression equations for these analyses were: (BF volume = $0.001479 - 3.498e-005 \times TNFRSF10B$; $R^2 = 0.00$; $P = 0.9$), (BF volume = $0.0015 - 0.0001456 \times CASP2$; $R^2 = 0.00$; $P = 0.8$), (BF volume = $0.001 - 0.0001173 \times BAX$; $R^2 = 0.00$; $P = 0.7$) and (BF volume = $0.0013 + 1.138e-005 \times CASP3$; $R^2 = 0.00$; $P = 0.7$).

Discussion

The observed discrepancies in the alignment of BF-DNA with TE and ICM samples across various studies highlight

the critical need to understand BF-DNA dynamics and the mechanisms underlying its formation (Farra et al. 2018). This understanding is essential for developing reliable and accurate less invasive preimplantation genetic methods. The mechanism of self-correction in mosaic embryos is a theoretical concept suggesting the ability of human embryos to eliminate abnormal cells from blastocysts, with evidence suggesting that approximately 70% of aneuploid embryos transition from cleavage-stage to euploid blastocysts during early embryogenesis, which strengthens the hypothesis of selective elimination of abnormal cells during blastocyst formation (Tobler et al. 2015). Furthermore, using a mouse model, it has been shown that aneuploid cells are preferentially eliminated from the embryonic lineage. This process involves autophagy and apoptosis before, during and after implantation. Meanwhile, diploid cells in mosaic embryos proliferate during implantation to compensate for this loss (Singla et al. 2020).

In line with the hypothesis that aneuploid cells may be eliminated from human blastocysts through apoptotic

mechanisms, we designed the present study (see Graphical Abstract). Our findings indicated that overexpression of apoptotic genes *TNFRSF10B*, *CASP2*, *CASP3* and high levels of BF-DNA in the blastocoel cavity correlate with the grade of aneuploidy. This suggests that embryos with more complex aneuploidy release higher levels of BF-DNA through apoptosis. Our findings support the idea that apoptosis may be a mechanism that leads to the removal of aneuploid cells from human blastocysts. It appears that the BF-DNA amount is influenced by the aneuploidy status and the number of chromosomes involved in aneuploidy. In addition, it should be considered that the size of chromosomal aberrations can lead to heterogeneity. In this context, our results revealed a higher amount of BF-DNA (114 ng/ μ L) in one of the female embryos in the SE group with partial aneuploidy compared to other embryos in the same group. Using array CGH, a gain of approximately 30 megabases on chromosome 7: 7q11.23-q22.1 in this blastocyst was identified (Supplementary Table 1). This finding highlights how the size of the chromosomal aberration may impact the embryo's response to aneuploidy, particularly at a partial level. The assumption is that a gene dose defect causes an imbalanced protein reservoir and proteotoxic stress, as well as replication stress that can lead to DNA damage and apoptotic cell death in aneuploid cells (Regin *et al.* 2024).

A study on survival signals and apoptosis in preimplantation embryos showed that the genes *CASP3*, *CASP2* and *TNFRSF10B* are expressed in both human and mouse blastocysts (Haouzi *et al.* 2018). The role of *TNFRSF10B* in cancer cell apoptosis has been shown to activate *CASP3* in human lung cancer cells (Zhao *et al.* 2014). Our study found upregulation of *TNFRSF10B* and *CASP3* genes in blastocysts with more complex aneuploidies compared to SEs. It seems that abnormal embryo growth is associated with changes in the expression level of *CASP3* (Regin *et al.* 2022). Recently, a positive correlation between *CASP3* activity and cfDNA concentration in BF was reported (Rule *et al.* 2018). Interestingly, we observed that the *BAX* gene is downregulated in blastocysts of FSDA and MA groups, in comparison with SEs. This observation aligns with previous research, which reported reduced *BAX* expression in aneuploid blastocysts in comparison with euploid blastocysts (Ahmed *et al.* 2023). It was reported that the presence of an extra chromosome 21 may elevate oxidative stress even at early developmental stages (Licciardi *et al.* 2018). The *BAX* gene regulates mitochondrial apoptosis through a balance with anti-apoptotic factors such as *BCL2*, which are influenced by mRNA and post-translational modifications (Dome *et al.* 2022). However, due to the lack of data on *BCL2* expression in our study, the impact of *BAX* in relation to its balance with *BCL2* remains unclear.

Embryo morphology has long been used in assisted reproductive technology centers to enhance outcomes,

but studies on day-5 embryos reveal that even those with good morphology may still be aneuploid (Rienzi *et al.* 2015, Fesahat *et al.* 2017). This indicates that morphology alone is not a reliable method for selecting chromosomally normal embryos. Therefore, we examined day-5 embryo morphology in relation to its chromosomal status, as previous research indicated that embryos with better morphology have higher concentrations of cfDNA in BF (Rule *et al.* 2018). In contrast, we did not observe a correlation between BF-DNA concentration and embryo morphological score. This discrepancy may be due to differences in study criteria; Rule *et al.* (2018) did not report the ploidy status of their embryos, whereas we included blastocysts based on their ploidy status. In addition, our study used the REPLI-g single-cell kit (QIAGEN, USA) to amplify BF-DNA and the Qubit device to measure very low DNA quantities precisely. In contrast, Rule *et al.* (2018) quantified DNA without amplification, using a NanoDrop 3300 fluorospectrometer, which may explain the observed differences in results.

The limitations of our study that may have influenced our findings are as follows: a primary limitation was the small sample size of analyzed embryos. Access to embryos with a normal chromosomal status was restricted due to ethical committee regulations. Furthermore, the small volume of BF collected ($\sim 0.001 \mu$ L) and its degraded nature may have impacted the upstream processes. However, as mentioned in the Materials and methods section, to minimize BF loss, the ICSI needles were broken into the vials and sample collection was optimized based on previous reports (Magli *et al.* 2016, Campos & Nel-Themaat 2024). The WGA technology, which can amplify short and degraded DNA fragments, was employed to amplify BF-DNA; however, DNA fragmentation into smaller pieces can affect primer sequence functionality and may interfere with PCR-based amplification. In addition, the freezing of embryos could potentially cause cellular damage, leading to the release of cellular DNA into the BF. However, this is unlikely to have affected our study, as vitrification was used, which causes less cellular damage than slow freezing methods (Li *et al.* 2012, Nagy *et al.* 2020, Vining *et al.* 2021).

Currently, the most effective method for embryo freezing involves the removal of BF to prevent ice crystal formation and protect the blastocyst. Clinical evidence has shown that this approach is highly effective in maintaining embryo viability (Kovačić *et al.* 2022, Umair *et al.* 2023). Therefore, BF obtained during embryo freezing presents a promising area for less invasive genetic analysis of embryos, without incurring additional costs for patients and clinics.

Our investigation showed that the BF-DNA level in blastocysts is dependent on the degree of aneuploidy, and the BF-DNA present is likely associated with apoptosis mechanisms during pre-implantation embryo development. Based on the results of this study and

other research, although BF-based methods are still in their early stages of development, optimizing BF-DNA isolation and amplification protocols to overcome challenges such as degradation and fragmentation could enhance the reliability of these methods. Our findings may contribute to improving the selection of suitable embryos for transfer with the most implantation potential through scoring based on the amount of BF-DNA released into the blastocoel cavity. Future studies with larger sample sizes, comparing normal and aneuploid embryos, as well as fresh and frozen embryos, are recommended to further evaluate the potential of this method.

Supplementary materials

This is linked to the online version of the paper at <https://doi.org/10.1530/RAF-24-0097>.

Declaration of interest

The authors declare that there is no conflict of interest that could be perceived as prejudicing the impartiality of the research reported.

Funding

This study was funded by the Royan Institute (Tehran, Iran) (project code: 99000154).

Data availability

The data underlying this article can be obtained by contacting the corresponding author.

Author contribution statement

FK, MB, ZN, HG and PE contributed to the conceptualization and methodology of the study. FK, PE, SH and RP were involved in the investigation and resource management. FK, MB, ZN and RP contributed to data analysis. FK was responsible for writing the original draft of the manuscript. FK, ZN, MB and HG reviewed and edited the manuscript. MB managed the project administration. FK and MB acquired funding for the study. All authors have read and approved the final manuscript.

Ethical considerations

This study was performed in line with the principles of the Declaration of Helsinki. Approval was granted by the Institutional Research Ethics Committee (approval code: IR.ACECR.ROYAN.REC.1400.094).

Acknowledgments

The authors are grateful to all of the patients who agreed to donate their embryos for research. They also thank Reza Mohammadi and Morteza Kimiai for technical assistance.

References

Ahmed M, Aytaçoglu H, Coban O, *et al.* 2023 Investigation of BAK, BAX and MAD2L1 gene expression in human aneuploid blastocysts. *Zygote* **31** 605–611. (<https://doi.org/10.1017/s0967199423000539>)

Boeddeker SJ & Hess AP 2015 The role of apoptosis in human embryo implantation. *J Reprod Immunol* **108** 114–122. (<https://doi.org/10.1016/j.jri.2015.02.002>)

Bolton H, Graham SJ, Van der Aa N, *et al.* 2016 Mouse model of chromosome mosaicism reveals lineage-specific depletion of aneuploid cells and normal developmental potential. *Nat Commun* **7** 11165. (<https://doi.org/10.1038/ncomms11165>)

Braude P 2018 The emperor still looks naked. *Reprod Biomed Online* **37** 133–135. (<https://doi.org/10.1016/j.rbmo.2018.06.018>)

Bustin SA, Benes V, Garson JA, *et al.* 2009 The MIQE guidelines: minimum information for publication of quantitative real-time PCR experiments. *Clin Chem* **55** 611–622. (<https://doi.org/10.1373/clinchem.2008.112797>)

Campos G & Nel-Themaat L 2024 Blastocoel fluid as an alternative source of DNA for minimally invasive PGT and biomarker of embryo competence. *Reprod Biomed Online* **49** 104322. (<https://doi.org/10.1016/j.rbmo.2024.104322>)

Capalbo A, Ubaldi FM, Rienzi L, *et al.* 2017 Detecting mosaicism in trophectoderm biopsies: current challenges and future possibilities. *Hum Reprod* **32** 492–498. (<https://doi.org/10.1093/humrep/dew250>)

Capalbo A, Poli M, Rienzi L, *et al.* 2021 Mosaic human preimplantation embryos and their developmental potential in a prospective, non-selection clinical trial. *Am J Hum Genet* **108** 2238–2247. (<https://doi.org/10.1016/j.ajhg.2021.11.002>)

Cimadomo D, Capalbo A, Ubaldi FM, *et al.* 2016 The impact of biopsy on human embryo developmental potential during preimplantation genetic diagnosis. *BioMed Res Int* **2016** 7193075. (<https://doi.org/10.1155/2016/7193075>)

Dome A, Dymova M, Richter V, *et al.* 2022 Post-transcriptional modifications of RNA as regulators of apoptosis in glioblastoma. *Int J Mol Sci* **23** 9272. (<https://doi.org/10.3390/ijms23169272>)

Farra C, Choucair F & Awwad J 2018 Non-invasive pre-implantation genetic testing of human embryos: an emerging concept. *Hum Reprod* **33** 2162–2167. (<https://doi.org/10.1093/humrep/dey314>)

Fesahat F, Montazeri F, Sheikhha MH, *et al.* 2017 Frequency of chromosomal aneuploidy in high quality embryos from young couples using preimplantation genetic screening. *Int J Reprod BioMedicine* **15** 297–304. (<https://doi.org/10.29252/ijrm.15.5.297>)

Fragouli E, Alfarawati S, Daphnis DD, *et al.* 2011 Cytogenetic analysis of human blastocysts with the use of FISH, CGH and aCGH: scientific data and technical evaluation. *Hum Reprod* **26** 480–490. (<https://doi.org/10.1093/humrep/deq344>)

Fragouli E, Alfarawati S, Spath K, *et al.* 2017 Analysis of implantation and ongoing pregnancy rates following the transfer of mosaic diploid–aneuploid blastocysts. *Hum Genet* **136** 805–819. (<https://doi.org/10.1007/s00439-017-1797-4>)

Franasiak JM, Forman EJ, Hong KH, *et al.* 2014 The nature of aneuploidy with increasing age of the female partner: a review of 15,169 consecutive trophectoderm biopsies evaluated with comprehensive chromosomal screening. *Fertil Steril* **101** 656–663.e1. (<https://doi.org/10.1016/j.fertnstert.2013.11.004>)

Gardner DK, Lane M & Schoolcraft WB 2002 Physiology and culture of the human blastocyst. *J Reprod Immunol* **55** 85–100. ([https://doi.org/10.1016/s0165-0378\(01\)00136-x](https://doi.org/10.1016/s0165-0378(01)00136-x))

Gianaroli L, Albanese C, Tabanelli C, *et al.* 2019 Blastocoel fluid biopsy. *Fertil & Reprod* **01** 17–20. (<https://doi.org/10.1142/s2661318219300034>)

Gleicher N & Orvieto R 2017 Is the hypothesis of preimplantation genetic screening (PGS) still supportable? A review. *J Ovarian Res* **10** 21. (<https://doi.org/10.1186/s13048-017-0318-3>)

Greco E, Minasi MG & Fiorentino F 2015 Healthy babies after intrauterine transfer of mosaic aneuploid blastocysts. *N Engl J Med* **373** 2089–2090. (<https://doi.org/10.1056/nejmc1500421>)

- Haouzi D, Boumela I, Chebli K, *et al.* 2018 Global, survival, and apoptotic transcriptome during mouse and human early embryonic development. *BioMed Res Int* **2018** 5895628. (<https://doi.org/10.1155/2018/5895628>)
- Hawke DC, Watson AJ & Betts DH 2021 Extracellular vesicles, microRNA and the preimplantation embryo: non-invasive clues of embryo well-being. *Reprod Biomed Online* **42** 39–54. (<https://doi.org/10.1016/j.rbmo.2020.11.011>)
- Hu Z, Chen H, Long Y, *et al.* 2021 The main sources of circulating cell-free DNA: apoptosis, necrosis and active secretion. *Crit Rev Oncol Hematol* **157** 103166. (<https://doi.org/10.1016/j.critrevonc.2020.103166>)
- Kovačić B, Taborin M, Vlaisavljević V, *et al.* 2022 To collapse or not to collapse blastocysts before vitrification? A matched case-control study on single vitrified-warmed blastocyst transfers. *Reprod Biomed Online* **45** 669–678. (<https://doi.org/10.1016/j.rbmo.2022.03.030>)
- Leaver M & Wells D 2020 Non-invasive preimplantation genetic testing (niPGT): the next revolution in reproductive genetics? *Hum Reprod Update* **26** 16–42. (<https://doi.org/10.1093/humupd/dmz033>)
- Li L, Zhang X, Zhao L, *et al.* 2012 Comparison of DNA apoptosis in mouse and human blastocysts after vitrification and slow freezing. *Mol Reprod Dev* **79** 229–236. (<https://doi.org/10.1002/mrd.22018>)
- Licciardi F, Lhakhang T, Kramer YG, *et al.* 2018 Human blastocysts of normal and abnormal karyotypes display distinct transcriptome profiles. *Sci Rep* **8** 14906. (<https://doi.org/10.1038/s41598-018-33279-0>)
- Lledó B, Morales R, Ortiz JA, *et al.* 2017 Implantation potential of mosaic embryos. *Syst Biol Reprod Med* **63** 206–208. (<https://doi.org/10.1080/19396368.2017.1296045>)
- Macklon NS, Ahuja KK & Fauser BCJM 2019 Building an evidence base for IVF 'add-ons'. *Reprod Biomed Online* **38** 853–856. (<https://doi.org/10.1016/j.rbmo.2019.04.005>)
- Magli MC, Pomante A, Cafueri G, *et al.* 2016 Preimplantation genetic testing: polar bodies, blastomeres, trophectoderm cells, or blastocoelic fluid? *Fertil Steril* **105** 676–683.e5. (<https://doi.org/10.1016/j.fertnstert.2015.11.018>)
- Maxwell SM & Grifo JA 2018 Should every embryo undergo preimplantation genetic testing for aneuploidy? A review of the modern approach to in vitro fertilization. *Best Pract Res Clin Obstet Gynaecol* **53** 38–47. (<https://doi.org/10.1016/j.bpobgyn.2018.07.005>)
- Michailov Y, Friedler S & Saar-Ryss B 2023 Methods to improve frozen-thawed blastocyst transfer outcomes-the IVF laboratory perspective. *J IVF-Worldwide* **1** 1–15. (<https://doi.org/10.46989/001c.87541>)
- Nagy ZP, Shapiro D & Chang CC 2020 Vitrification of the human embryo: a more efficient and safer in vitro fertilization treatment. *Fertil Steril* **113** 241–247. (<https://doi.org/10.1016/j.fertnstert.2019.12.009>)
- Popovic M Losing balance: investigating the prevalence and impact of chromosomal instability during early human development. *Doctoral Dissertation* 2019. Ghent University.
- Regin M, Spits C & Sermon K 2022 On the origins and fate of chromosomal abnormalities in human preimplantation embryos: an unsolved riddle. *Mol Hum Reprod* **28** gaac011. (<https://doi.org/10.1093/molehr/gaac011>)
- Regin M, Lei Y, De Deckersberg EC, *et al.* 2024 Complex aneuploidy triggers autophagy and p53-mediated apoptosis and impairs the second lineage segregation in human preimplantation embryos. *eLife* **12** RP88916. (<https://doi.org/10.7554/eLife.88916.3>)
- Rienzi L, Capalbo A, Stoppa M, *et al.* 2015 No evidence of association between blastocyst aneuploidy and morphokinetic assessment in a selected population of poor-prognosis patients: a longitudinal cohort study. *Reprod Biomed Online* **30** 57–66. (<https://doi.org/10.1016/j.rbmo.2014.09.012>)
- Rubio C, Rodrigo L & Simón C 2020 Preimplantation genetic testing: chromosome abnormalities in human embryos. *Reproduction* **160** A33–A44. (<https://doi.org/10.1530/rep-20-0022>)
- Rule K, Chosed RJ, Arthur Chang T, *et al.* 2018 Relationship between blastocoel cell-free DNA and day-5 blastocyst morphology. *J Assist Reprod Genet* **35** 1497–1501. (<https://doi.org/10.1007/s10815-018-1223-4>)
- Sauer MV 2015 Reproduction at an advanced maternal age and maternal health. *Fertil Steril* **103** 1136–1143. (<https://doi.org/10.1016/j.fertnstert.2015.03.004>)
- Schattman GL 2018 Chromosomal mosaicism in human preimplantation embryos: another fact that cannot be ignored. *Fertil Steril* **109** 54–55. (<https://doi.org/10.1016/j.fertnstert.2017.11.022>)
- Sermon K, Capalbo A, Cohen J, *et al.* 2016 The why, the how and the when of PGS 2.0: current practices and expert opinions of fertility specialists, molecular biologists, and embryologists. *MHR: Basic Sci Reprod Med* **22** 845–857. (<https://doi.org/10.1093/molehr/gaw034>)
- Singla S, Iwamoto-Stohl LK, Zhu M, *et al.* 2020 Autophagy-mediated apoptosis eliminates aneuploid cells in a mouse model of chromosome mosaicism. *Nat Commun* **11** 2958. (<https://doi.org/10.1038/s41467-020-16796-3>)
- Tiwari M, Prasad S, Tripathi A, *et al.* 2015 Apoptosis in mammalian oocytes: a review. *Apoptosis* **20** 1019–1025. (<https://doi.org/10.1007/s10495-015-1136-y>)
- Tobler KJ, Zhao Y, Ross R, *et al.* 2015 Blastocoel fluid from differentiated blastocysts harbors embryonic genomic material capable of a whole-genome deoxyribonucleic acid amplification and comprehensive chromosome microarray analysis. *Fertil Steril* **104** 418–425. (<https://doi.org/10.1016/j.fertnstert.2015.04.028>)
- Umair M, Beitsma M, de Ruijter-Villani M, *et al.* 2023 Vitrifying expanded equine embryos collapsed by blastocoel aspiration is less damaging than slow-freezing. *Theriogenology* **202** 28–35. (<https://doi.org/10.1016/j.theriogenology.2023.02.028>)
- Vera-Rodriguez M, Chavez SL, Rubio C, *et al.* 2015 Prediction model for aneuploidy in early human embryo development revealed by single-cell analysis. *Nat Commun* **6** 7601. (<https://doi.org/10.1038/ncomms8601>)
- Vining LM, Zak LJ, Harvey SC, *et al.* 2021 The role of apoptosis in cryopreserved animal oocytes and embryos. *Theriogenology* **173** 93–101. (<https://doi.org/10.1016/j.theriogenology.2021.07.017>)
- Zhao X, Liu X & Su L 2014 Parthenolide induces apoptosis via TNFRSF10B and PMAIP1 pathways in human lung cancer cells. *J Exp Clin Cancer Res* **33** 3–11. (<https://doi.org/10.1186/1756-9966-33-3>)